

Supporting Information

K(Gd_{0.1}Yb_{0.9})₃F₁₀, A Promising Refrigerant for sub-100 mK Adiabatic Demagnetization Refrigeration

Qiao-Fei Xu,^{ab,#} Peng Zhao,^{c,#} Man-Ting Chen,^a Ruo-Tong Wu,^a Wei Dai,^{c,} La-Sheng Long,^{a,*} and Lan-Sun Zheng^a*

^a Collaborative Innovation Center of Chemistry for Energy Materials, State Key Laboratory of Physical Chemistry of Solid Surfaces, College of Chemistry and Chemical Engineering, Xiamen University, Xiamen 361005, China

E-mail: lslong@xmu.edu.cn

^b Key Laboratory of Functional Molecular Solids Ministry of Education, College of Chemistry and Materials Science, Anhui Normal University, Wuhu, 241002, Anhui, China.

^c State Key Laboratory of Cryogenic Science and Technology, Technical Institute of Physics and Chemistry, Chinese Academy of Sciences, Beijing 100190, China

E-mail: cryodw@mail.ipc.ac.cn

Q.-F. Xu and P. Zhao contributed equally to this work.

Measurement and methods: All materials including $\text{Gd}_2(\text{SO}_4)_3 \cdot 8\text{H}_2\text{O}$, reagents, and solvents were commercially sourced and used without further purification. Powder X-ray diffraction (XRD) data were collected using a Rigaku Ultima IV X-ray diffractometer with $\text{Cu K}\alpha$ radiation. The proportion of Gd and Yb in **1** were evaluated using an Agilent 7800 ICP-MS, with results reported as the average of three measurements. Elemental mapping of **1** was performed with a ZEISS Sigma scanning electron microscope. Magnetic susceptibility was measured with a Quantum Design superconducting quantum interference device (SQUID). Heat capacity was investigated using a Quantum Design physical property measurement system.

X-ray Crystallography: Data of **1** was collected using an XtaLAB Synergy four-circle diffractometer with monochromatic $\text{Mo K}\alpha$ radiation. Data reduction and absorption correction were applied by using the multi-scan program. The structures were determined and refined using full-matrix least-squares based on F^2 with SHELXS and SHELXL-2018¹ within Olex2.² Crystal data and refinement details are presented in Table S1. The data can be obtained free of charge from the FIZ Karlsruhe (CSD 2523489).

The two-stage refrigerator: Fig. 3a illustrates the two-stage ADR used in this study, which consists of a 2nd cold plate (heat sink), two magnets capable of providing a maximum magnetic field of 4 T, a GGG salt pill, a **1** salt pill, and two heat switches. The two salt pills are each installed within their respective magnets. The **1** salt pill is connected to the GGG salt pill via HS2, while the GGG salt pill is connected to the 2nd cold plate via HS1. Thermometers are mounted on both salt pills, and a resistive heater is attached to the **1** salt pill to apply a heat load. The cooling process operates as follows: First, with HS1 turned off and HS2 turned on, the GGG salt pill is demagnetized to pre-cool the **1** salt pill. After the pre-cooling is completed, HS2 is turned off, and then the **1** salt pill is demagnetized.

The two heat switches used in the experiment are active gas-gap heat switches, with their structure shown in Fig. S5. Each heat switch consists of an adsorption bed containing adsorbent material (activated carbon) and a main body. The main body is composed of two heat transfer copper fins that are not in direct contact and form a gas-gap space, along with a stainless steel sealing shell. The interior of the heat switch is filled with a certain amount of ³He gas, typically

on the order of 10^{-4} g, with a cost of a few dollars. At low temperatures, the ^3He gas is adsorbed by the adsorbent material, leaving the gas gap in a high-vacuum state, and the heat switch is in the off state. When heat is applied to the adsorption bed, the ^3He gas adsorbed in the adsorbent material desorbs and enters the gas gap, transitioning the heat switch to the on state.

Table S1 Crystal data for **1**

Compound	1
Formula	$\text{K}(\text{Gd}_{0.1}\text{Yb}_{0.9})_3\text{F}_{10}$
Formula weight	743.48
Temperature/K	100
Crystal system	Cubic
Space group	$Fm\bar{3}m$
$a/\text{\AA}$	11.4254(3)
$V/\text{\AA}^3$	1491.47(10)
Z	8
$D_c/\text{g cm}^{-3}$	6.622
μ/mm^{-1}	36.917
$2\theta^\circ$	7.132-58.006
Independent reflections	126
$F(000)$	2538
GOOF	1.202
$R_1[I > 2\sigma(I)]^a$	0.0133
$wR_2(\text{All data})^b$	0.0493

$$^a R_1 = \sum ||F_o| - |F_c|| / \sum |F_o| \quad ^b wR_2 = \{ \sum [w(F_o^2 - F_c^2)^2] / \sum [w(F_o^2)^2] \}^{1/2}$$

Table S2. ICP results in **1, $\text{K}(\text{Lu}_{0.9}\text{Gd}_{0.1})_3\text{F}_{10}$ and $\text{K}(\text{Yb}_{0.9}\text{Y}_{0.1})_3\text{F}_{10}$.**

	Experimental value	Calculated value
	Yb : Gd	
1	9.02 ± 0.05	9.0
	Lu : Gd	
$\text{K}(\text{Lu}_{0.9}\text{Gd}_{0.1})_3\text{F}_{10}$	8.98 ± 0.06	9.0
	Yb : Y	
$\text{K}(\text{Yb}_{0.9}\text{Y}_{0.1})_3\text{F}_{10}$	9.05 ± 0.09	9.0

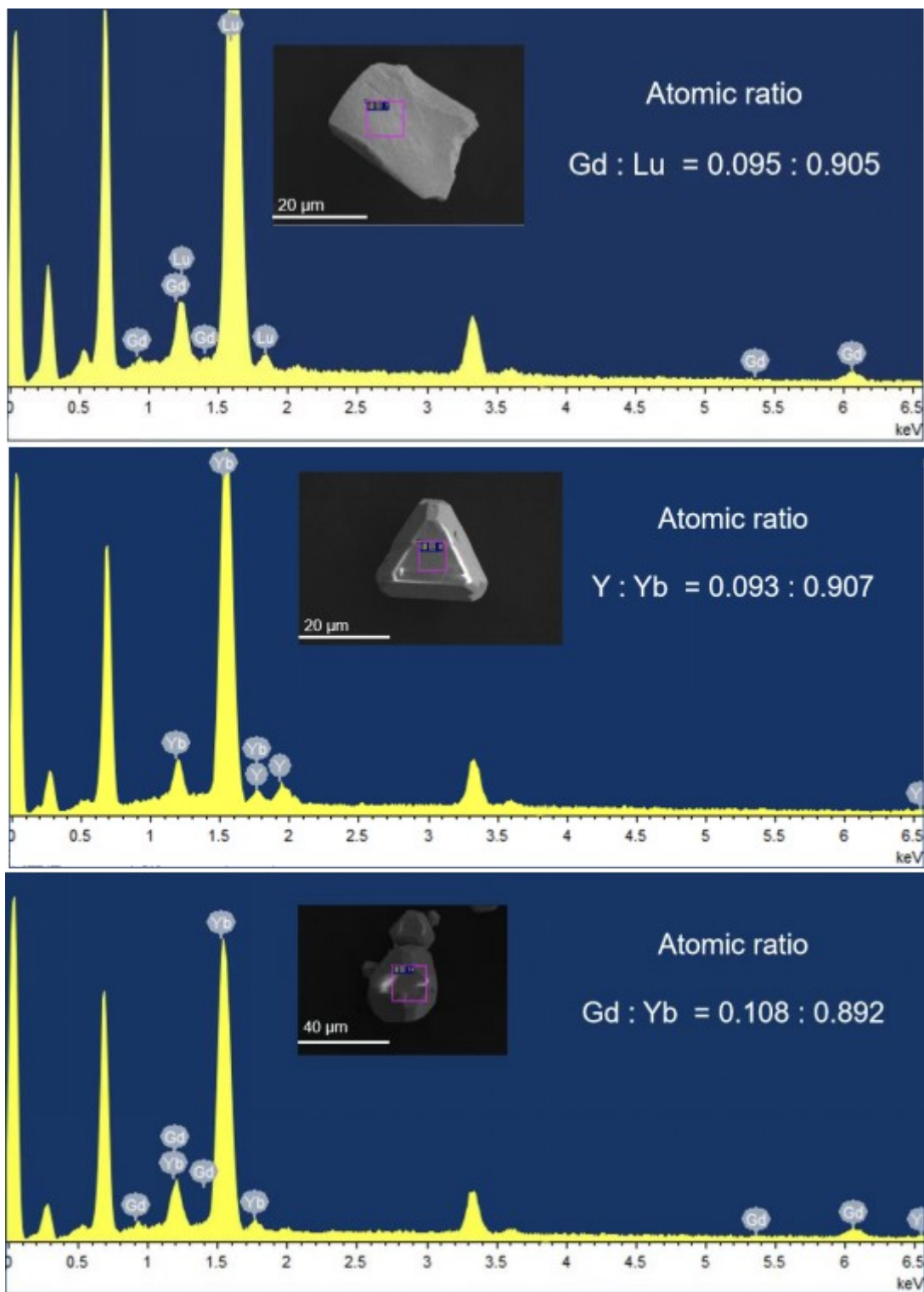


Fig. S1. Energy-dispersive X-ray spectroscopy of $\text{K}(\text{Lu}_{0.9}\text{Gd}_{0.1})_3\text{F}_{10}$ and $\text{K}(\text{Yb}_{0.9}\text{Y}_{0.1})_3\text{F}_{10}$ and **1**.

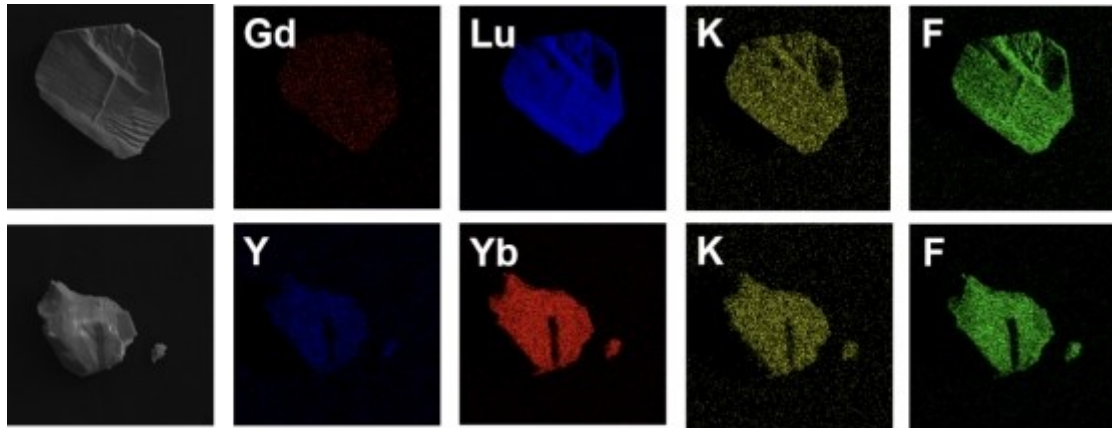


Fig. S2. EDS elemental maps of $\text{K}(\text{Lu}_{0.9}\text{Gd}_{0.1})_3\text{F}_{10}$ and $\text{K}(\text{Yb}_{0.9}\text{Y}_{0.1})_3\text{F}_{10}$.

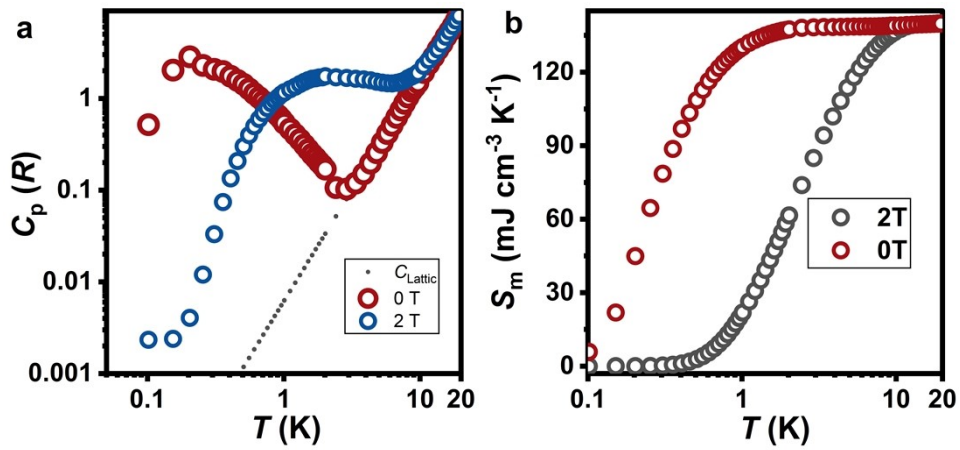


Fig. S3 (a) Experimental heat capacity (C_p) normalized to the gas constant (R) of $\text{Gd}_2(\text{SO}_4)_3 \cdot 8\text{H}_2\text{O}$; (b) The experimental magnetic entropy S_m in $\text{Gd}_2(\text{SO}_4)_3 \cdot 8\text{H}_2\text{O}$ under various applied fields.

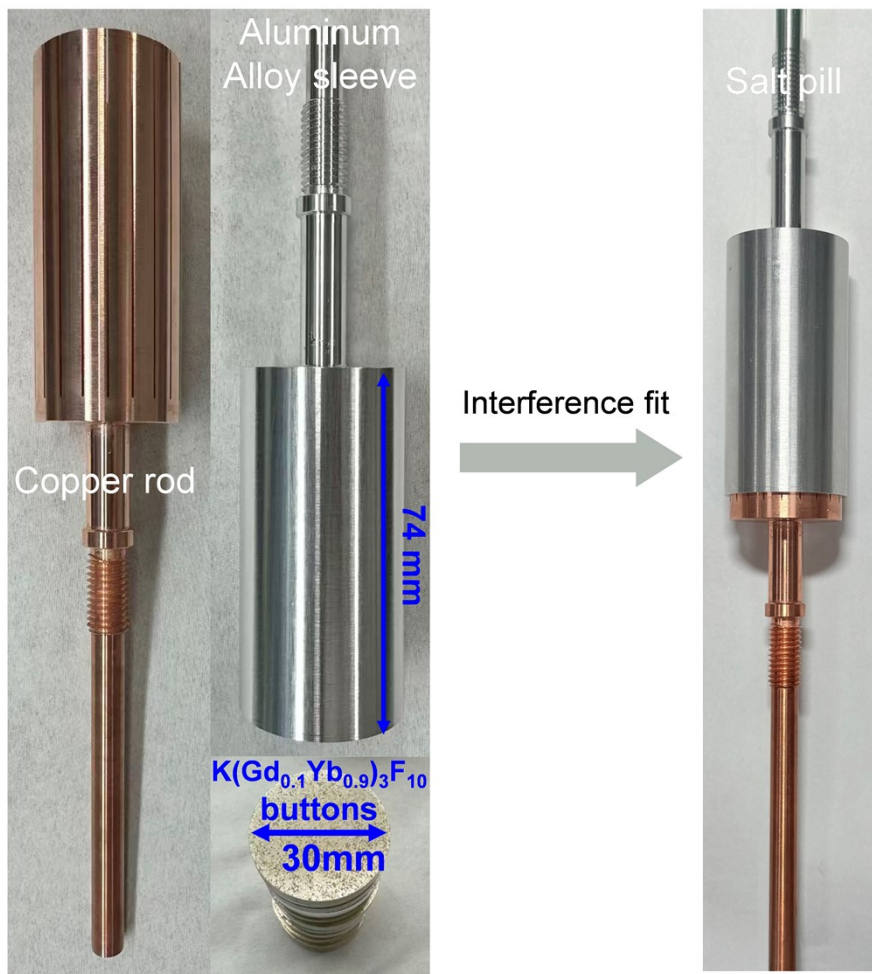


Fig. S4. Salt pill photos

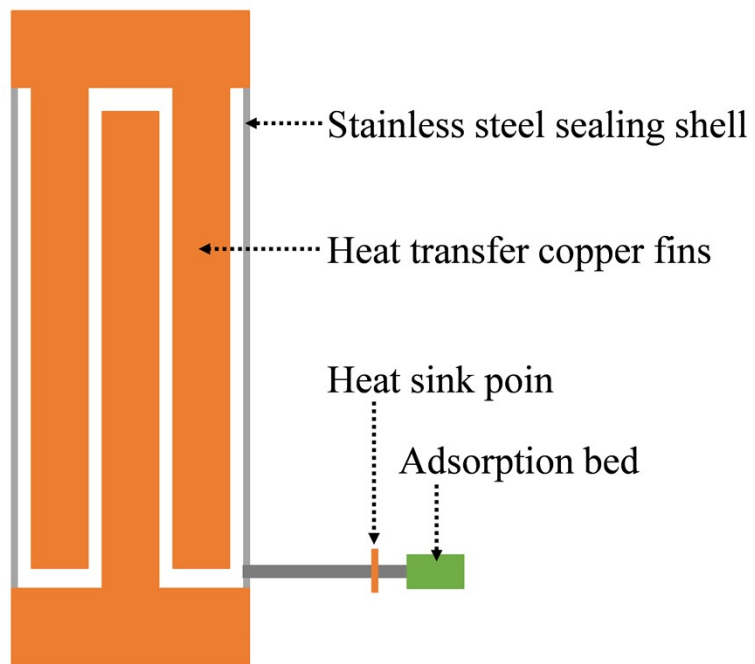


Fig. S5 Schematic diagram of thermal switch structure

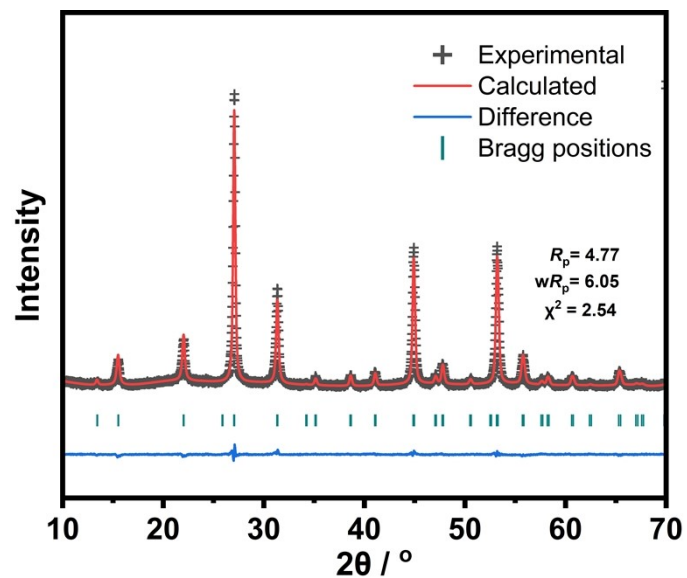


Fig. S6 PXR D of scale-up 1.

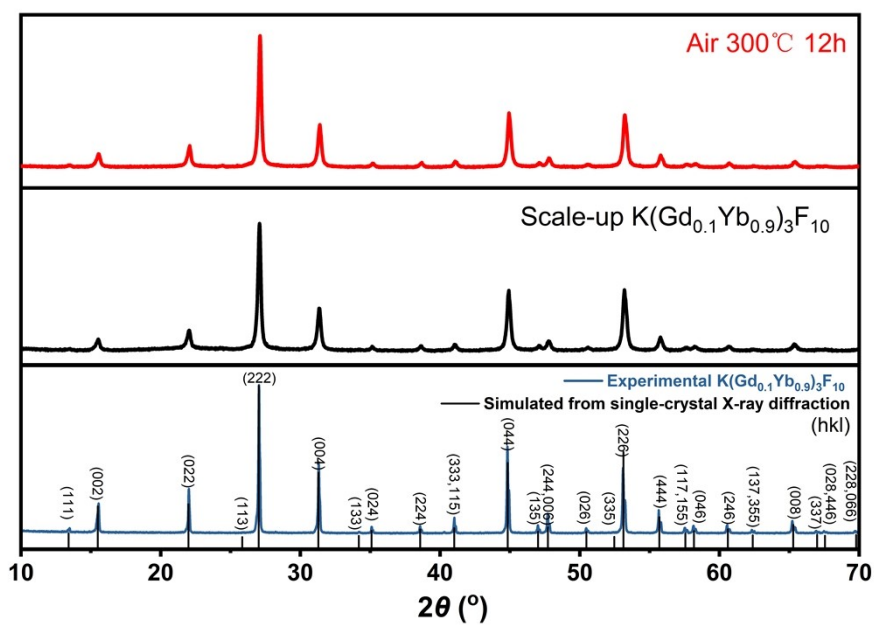


Fig. S7 PXR D of scale-up 1 and 1 under 300 °C after 6 h.

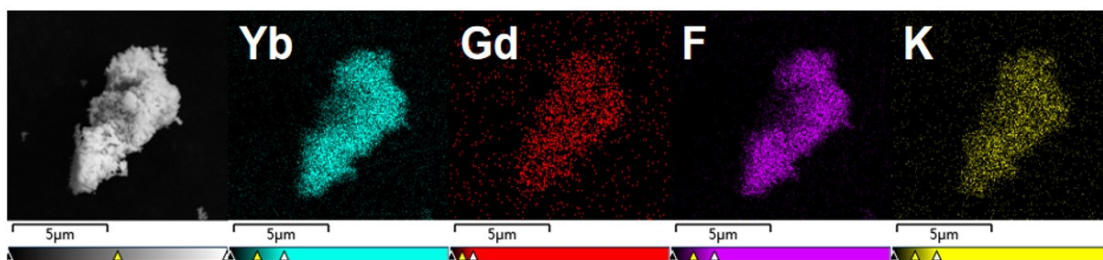


Fig. S8 Elemental mapping of scale-up 1.

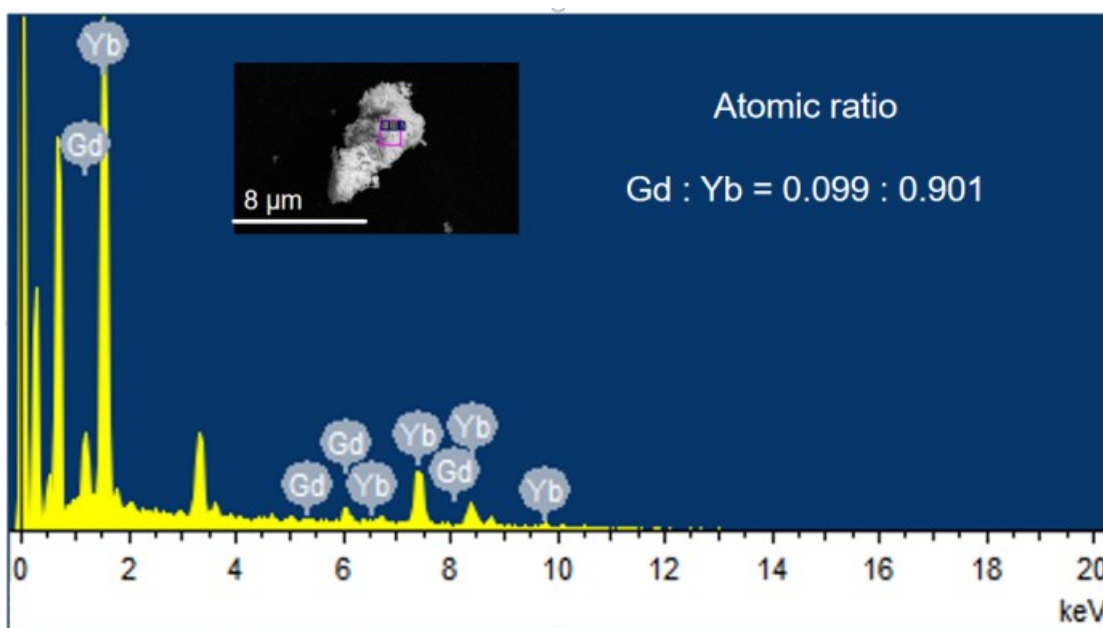


Fig. S9. Energy-dispersive X-ray spectroscopy of scale-up 1.

References

- 1 Sheldrick GM. *Acta Crystallogr Sect A Found Crystallogr* 2008, 64: 112–122.
- 2 Dolomanov OV, Bourhis LJ and Gildea RJ *et al. J Appl Crystallogr* 2009, 42: 339–341.